IJC
International Journal of Cancer

Targeted therapy of the AKT kinase inhibits esophageal squamous cell carcinoma growth *in vitro* and *in vivo*

Xuejiao Liu[1,2*], Mengqiu Song[1,2*], Penglei Wang[1,2*], Ran Zhao[1,2], Hanyong Chen[3], Man Zhang[2], Yuanyuan Shi[2], Kangdong Liu[1,2,4], Fangfang Liu[1,2], Ran Yang[2], Enmin Li[5], Ann M. Bode[3], Zigang Dong[1,2,3,4] and Mee-Hyun Lee[1,2,3]

[1]School of Basic Medical Sciences, Zhengzhou University, Zhengzhou, Henan, China
[2]China-US (Henan) Hormel Cancer Institute, Zhengzhou, Henan, China
[3]The Hormel Institute, University of Minnesota, Austin, Minnesota
[4]The Collaborative Innovation Center of Henan Province for Cancer Chemoprevention, Zhengzhou, Henan, China
[5]Department of Biochemistry and Molecular Biology, Shantou University Medical College, Shantou, Guangdong, China

Esophageal cancer, a leading cause of cancer death worldwide, is associated with abnormal activation of the AKT signaling pathway. Xanthohumol, a prenylated flavonoid tested in clinical trials, is reported to exert anti-diabetes, anti-inflammation and anticancer activities. However, the mechanisms underlying its chemopreventive or chemotherapeutic effects remain elusive. In the present study, we found that xanthohumol directly targeted AKT1/2 in esophageal squamous cell carcinoma (ESCC). Xanthohumol significantly inhibited the AKT kinase activity in an ATP competitive manner, which was confirmed in binding and computational docking models. KYSE70, 450 and 510 ESCC cell lines highly express AKT and knockdown of AKT1/2 suppressed proliferation of these cells. Treatment with xanthohumol inhibited ESCC cell growth and induced apoptosis and cell cycle arrest at the G1 phase. Xanthohumol also decreased expression of cyclin D1 and increased the levels of cleaved caspase-3, -7 and -PARP as well as Bax, Bim_s and cytochrome *c* in ESCC cells by downregulating AKT signaling targets, including glycogen synthase kinase 3 beta (GSK3β), mammalian target of rapamycin, and ribosomal protein S6 (S6K). Furthermore, xanthohumol decreased tumor volume and weight in patient-derived xenografts (PDXs) that highly expressed AKT, but had no effect on PDXs that exhibited low expression of AKT *in vivo*. Kinase array results showed that xanthohumol treatment decreased phosphorylated p27 expression in both ESCC cell lines and PDX models. Taken together, our data suggest that the inhibition of ESCC tumor growth with xanthohumol is caused by targeting AKT. These results provide good evidence for translation toward clinical trials with xanthohumol.

Introduction

Esophageal cancer is one of the most aggressive and lethal malignancies worldwide, with a 5-year survival rate of around 10% for all patients.[1] The two major subtypes of esophageal cancer are esophageal squamous cell carcinoma (ESCC) and esophageal adenocarcinoma. ESCC accounts for 90% of all cases of esophageal cancer[2] and approximately 70% of esophageal cancer cases occur in China, with a higher incidence and mortality, especially in rural areas compared to urban areas.[3] Cancer statistics for China indicate that esophageal cancer is the 3rd and 5th most commonly diagnosed cancer among men and women, respectively.[4] Chemotherapy is a common method for treating esophageal cancer and drugs such as

Key words: targeting AKT kinase activity, xanthohumol, AKT signaling pathway, esophageal squamous cell carcinoma
Additional Supporting Information may be found in the online version of this article.
Conflict of Interest: The authors declare no conflicts of interest.
*X.L., M.S. and P.W. contributed equally to this work
[Correction added May 9 after first online publication: Affiliation was updated.]
Grant sponsor: Key program of Henan Province, China; **Grant number:** 161100510300; **Grant sponsor:** The National Institute of Health (NIH), USA; **Grant numbers:** CA 196639, CA187027; **Grant sponsor:** The National Natural Science Foundation of China; **Grant numbers:** NSFC81672767, 81802875
DOI: 10.1002/ijc.32285

History: Received 11 Oct 2018; Accepted 12 Mar 2019; Online 18 Mar 2019.
Correspondence to: Zigang Dong, The Hormel Institute, University of Minnesota, 801 16 Ave NE, Austin, MN 55912, USA, Tel.: +1-507-437-9600, Fax: +1-507-437-9606, E-mail: zgdong@hi.umn.edu; or Mee-Hyun Lee, China-US (Henan) Hormel Cancer Institute, No.127, Dongming Road, Jinshui District, Zhengzhou, Henan, 450008, China, Tel.: +86-371-65587008, Fax: +86-371-65587670, E-mail: mhlee@hci-cn.org; or mhyun_lee@hanmail.net

What's new?

Esophageal squamous cell carcinoma (ESCC) is among the most common and deadliest forms of esophageal malignancy. Chemotherapy remains the mainstay of treatment, even though many ESCC patients experience disease progression despite therapy. Here, the authors investigated a novel agent for ESCC, the prenylated flavonoid xanthohumol. In ESCC cells, xanthohumol was found to directly target AKT kinase, inhibiting AKT activity, suppressing cell proliferation, and inducing apoptosis. In a patient-derived xenograft mouse model, xanthohumol reduced tumor volume specifically in high AKT-expressing tumors, with little effect on low AKT tumors. The data suggest that AKT targeting is a promising therapeutic strategy in ESCC.

5-fluorouracil (5-FU), cisplatin, paclitaxel and mitomycin are commonly used to treat esophageal cancer as a single treatment or in combination.[5–8] In Asia, the first-line regimen of treating esophageal cancer is a combination therapy using fluoropyrimidine and platinum. In addition, a strategy of combining docetaxel, 5-FU, and cisplatin is used for young and fit patients.[9] However, this regimen causes substantial hematological toxicity.[10] The development of targeted therapies against esophageal cancer has not been progressing as rapidly or as smoothly as hoped over the past few decades. Drugs targeting epidermal growth factor receptor, vascular endothelial growth factor, human epidermal growth factor receptor 2, tyrosine-protein kinase MET, mammalian target of rapamycin (mTOR), or poly ADP ribose polymerase (PARP) have been investigated in clinical trials. However, most of the results have been disappointing[11] and new targets and inhibitors need to be identified for the treatment of esophageal cancer. AKT (also known as protein kinase B or PKB) is a serine/threonine-specific protein kinase and has been known for more than 25 years as an important node in cell signaling pathways.[12] AKT is reportedly deregulated in many kinds of cancers and is involved in various biological processes, including cell proliferation, apoptosis, transcription, migration and invasion.[13–15] About 15.7% of AKT1 amplification is found in ESCC[1] and at least one recent study demonstrated that the PI3-K/AKT signaling pathway plays an important role in ESCC metastasis.[16] Therefore, AKT should be a promising therapeutic target for treatment and control of ESCC.

Patient-derived xenograft (PDXs) models have been developed for translating basic research studies to clinical applications. To a large extent, the biological and genetic characteristics of a patient's donor tumor are believed to be preserved by PDX models, which offer advantages over cell line-based models. Furthermore, the characteristics of drug responsiveness and mutational status also can be passed from generation to generation.[17–19] Currently, PDX models are used to identify biomarkers and predict patient drug response in the clinic.[20–23]

Due to the multiple biological activities and relatively low systemic toxicity, natural anticancer products have gained attention from researchers. Xanthohumol is a prenylated flavonoid derived from the hop plant (*Humulus lupulus L*). It has shown antidiabetic, antiviral and antioxidative bioactivities[24] and a Phase I study with xanthohumol and its role in DNA damage is currently ongoing (NCT02432651). Xanthohumol also exhibited potential therapeutic effects against lung cancer,[25] breast cancer[26] and liver cancer.[27] Based on its inhibitory effects against cancer cell proliferation, migration and invasion, xanthohumol could be a promising drug for application in cancer treatment. In the present study, we demonstrate that xanthohumol inhibited ESCC cell proliferation and induced apoptosis and G1 cell cycle phase arrest. It also inhibited growth of PDXs. We found that the inhibitory activities of xanthohumol against ESCC are caused by directly targeting AKT kinase activity. These data suggest that xanthohumol is a promising therapeutic agent in ESCC chemotherapy.

Materials and Methods

Reagents

Xanthohumol (purity ≥97%) was purchased from Sichuan Weikeqi Biological Technology Co., Ltd (Chengdu, Sichuan, China). The active AKT1 and AKT2 recombinant proteins for kinase assays were purchased from SignalChem (Richmond, BC). Antibodies against phosphorylated AKT (p-AKT, Ser 473), AKT (pan), phosphorylated glycogen synthase kinase 3 beta (p-GSK3β, Ser 9), GSK3β, mTOR, p-S6K, cleaved PARP, cleaved Caspase 3, cleaved Caspase 7, Bax, Bim, cyclin D1, α-tubulin and COX IV were purchased from Cell Signaling Technology (Beverly, MA). Antibodies to detect cytochrome c, p-mTOR (Ser2448), or β-actin were purchased from Santa Cruz Biotechnology (Santa Cruz, CA) or Zhongshan Jinqiao Biological Technology Co., Ltd (Beijing, China). The Mitochondria/Cytosol Fractionation Kit was purchased from Biovision (Milpitas, CA).

Cell culture

The human ESCC cell lines, KYSE 30, KYSE70, KYSE 410, KYSE450 and KYSE510, were purchased from the Type Culture Collection of the Chinese Academy of Sciences (Shanghai, China). Cells were cultured in RPMI-1640 containing penicillin (100 units/ml), streptomycin (100 μg/ml) and 10% fetal bovine serum (FBS, Biological Industries, Kibbutz Beit-Haemek, Israel). The human immortalized normal esophageal epithelial cell line, SHEE (N1217), was donated by Dr. Enmin Li (Laboratory of Tumor Pathology, Shantou University Medical College).[28] Cells were maintained at 37°C in a humidified atmosphere with 5% CO_2. All cells were cytogenetically tested and authenticated before being frozen. Each vial of frozen cells was thawed and maintained in culture for a maximum of 10 passages.

Cell proliferation assay

Cells were seeded ($1.5–7 \times 10^3$ cells per well) in 96-well plates and then treated after 24 hr with different doses of xanthohumol. After 24, 48, or 72 hr of incubation, 20 μl of the MTT (4,5-dimethylthiazol-2-yl)-2,5-diphenyltetrazolium bromide, Ruitaibio, Beijing, China) reagent were added into each well. After 1 hr, medium was discarded

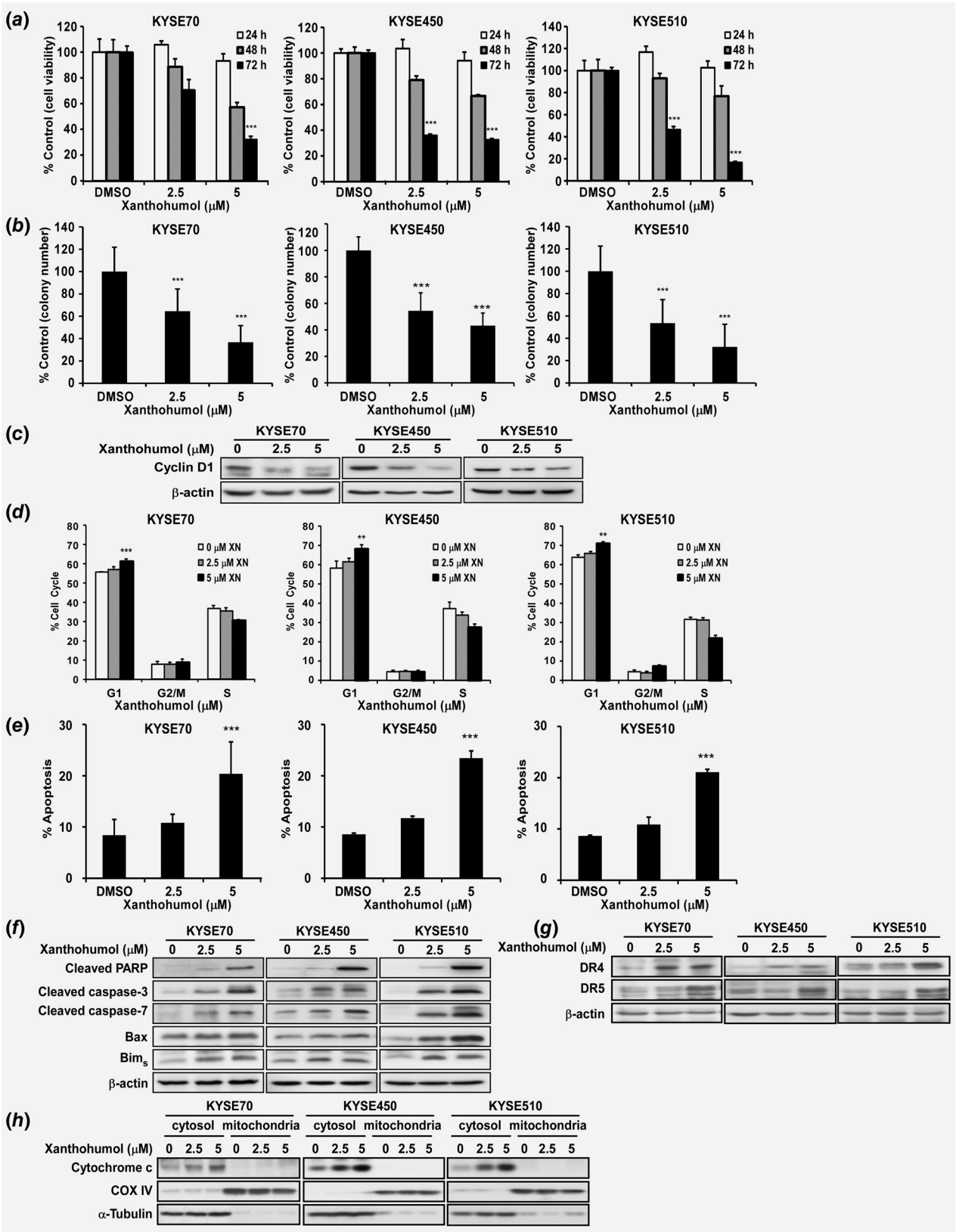

Figure 1. Legend on next page.

and 100 μl of DMSO (dimethyl sulfoxide, Sigma-Aldrich, St. Louis, MO) were added and absorbance was then measured at 570 nm using the Multiskan GO Microplate Spectrophotometer (Thermo Scientific, Vantaa, Finland).

Anchorage-independent cell growth

KYSE70, KYSE450, or KYSE510 cells were suspended in complete growth media and then 0.3% agar with different doses of xanthohumol was added in a top layer over a base layer of 0.5% agar. The cultures were maintained at 37°C in a 5% CO_2 incubator. Three weeks later, the colonies were counted and photographed under a microscope using the Image-Pro Plus software (v.6.0) program (Media Cybernetics, Rockville, MD).

Annexin V apoptosis assay

Cells were seeded in 60-mm dishes and treated with vehicle or 2.5 or 5 μM xanthohumol for 72 hr. Then cells were stained with annexin V (Biolegend, San Diego, CA) and propidium iodide (Solarbio, Beijing, China). After staining, cells were analyzed by a flow cytometer (FACSCalibur, BD Bioscience, San Jose, CA).

Cell cycle analysis

Cells were seeded in 60-mm dishes and treated with vehicle or 2.5 or 5 μM xanthohumol for 48 hr. Cells were fixed in 70% ethanol and stored at −20°C for 24 hr. After staining with propidium iodide, cell cycle was analyzed by flow cytometry (FACSCalibur, BD Bioscience, San Jose, CA).

Western blot assay

Cell lysates were prepared with lysis buffer (150 mM NaCl, 0.5–1% NP-40, 50 mM Tris–HCl, with 1 mM PMSF and protease inhibitor mixture) and quantified using the BCA Quantification Kit (Solarbio, Beijing, China). Proteins were subjected to 10–15% sodium dodecyl sulfate-polyacrylamide gel electrophoresis and transferred to a polyvinylidene difluoride membrane (Millipore, Billerica, MA). After blotting, the membrane was incubated with primary antibodies against specific targets, including p-AKT, AKT, p-mTOR, mTOR, p-GSK3β, GSK3β, p-S6K, or β-actin at 4°C overnight. Membranes were then incubated with the appropriate secondary antibody and the protein bands were visualized using the Amersham Image 600 (GE, Milwaukee, WI) imager.

Ex vivo pull-down assay

Xanthohumol-Sepharose 4B beads were prepared following the manufacturer's instructions (Amersharm Pharmacia Biotech, GE Healthcare Bio-Science, Uppsala, Sweden). Cell lysates were incubated with xanthohumol-Sepharose 4B beads or Sepharose 4B beads only in 1× lysis buffer (50 mM Tris–HCl pH 7.5, 5 mM EDTA, 150 mM NaCl, 1 mM dithiothreitol, 0.01% NP-40 and 2 mg/ml bovine serum albumin) at 4°C with rotation overnight. After incubation, the beads were washed 3 times with washing buffer (50 mM Tris–HCl pH 7.5, 5 mM EDTA, 150 mM NaCl, 1 mM dithiothreitol and 0.01% NP-40). AKT proteins bound to the beads were analyzed by Western blotting.

AKT kinase assay

Phospho-AKT (Ser473) (D9E) XP rabbit mAb (Sepharose bead-conjugate) and a GSK-3 fusion protein were purchased from Cell Signaling Technology. The AKT kinase assay was conducted following the protocol provided by Cell Signaling Technology. Cell lysates were incubated with phospho-AKT (Ser473)-conjugated Sepharose 4B beads and rotated overnight at 4°C. After washing with lysis buffer, ATP and the GSK-3 fusion protein were added and then incubated at 30°C for 30 min. Finally, the reaction was terminated with SDS sample buffer and proteins detected by Western blotting.

The ATP and xanthohumol competition assay

Active AKT1 or AKT2 was preincubated separately with 50 μl xanthohumol-Sepharose 4B beads in 1 × NETNL lysis buffer for 2 hr at 4°C. Then different concentrations of ATP (1, 10 or 100 μM) were added to a final volume of 1 ml and then incubated for another 2 hr. After incubation, the samples were washed as for the pull-down assay and proteins were detected by Western blotting.

Computational docking model

To further confirm that xanthohumol can bind with AKT, we performed an *in silico* docking assay using the Schrödinger Suite 2015 software programs.[29] The AKT1 and AKT2 crystal structures were first downloaded from the protein data bank (http://www.rcsb.org/pdb) and then prepared under the standard procedures of the Protein Preparation Wizard (Schrödinger Suite 2015). Hydrogen atoms were added consistent with a pH of 7 and all water molecules were removed. The ATP-binding site-based receptor grid was generated for docking. Xanthohumol was prepared for docking by default parameters using the LigPrep program. Then, the docking of xanthohumol with AKT1 and AKT2 was accomplished with default parameters under the extra precision (XP) mode using the program Glide. Herein, we could get the best-docked representative structures.

Figure 1. Xanthohumol inhibits esophageal cancer cell growth. (*a*) Cell proliferation was detected by MTT assay. Data show that xanthohumol inhibits ESCC cell growth in a dose-dependent manner. (*b*) Xanthohumol decreases colony formation in soft agar. Asterisks (*$p < 0.05$, **$p < 0.01$, ***$p < 0.001$) indicate a significant reduction in cancer cell growth and colony formation. (*c*) Xanthohumol reduces cyclin D1 as determined by Western blot analysis (48 hr post treatment). (*d*) Xanthohumol treatment leads to cell cycle arrest at the G1 phase at 48 hr. (*e*) Xanthohumol treatment increases apoptosis at 72 hr based on annexinV+/PI− gating. (*f–h*) Apoptotic protein markers are increased after xanthohumol treatment (Western blot detection at 72 hr post treatment). Asterisks (**$p < 0.01$, ***$p < 0.001$) indicate a significant change in cell cycle and apoptosis.

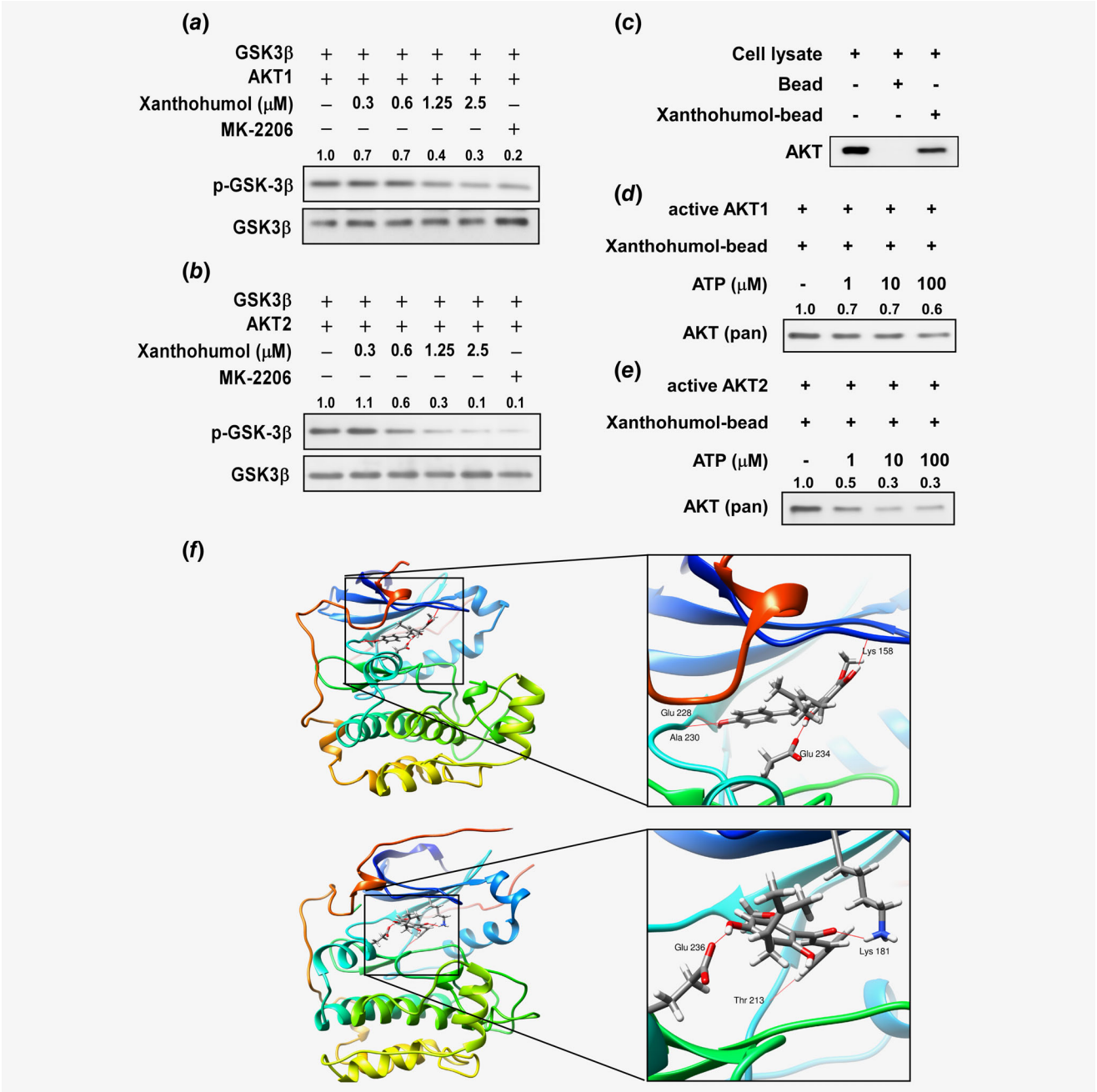

Figure 2. AKT is a target of xanthohumol. (*a*, *b*) Xanthohumol inhibits AKT kinase activity and downregulates the phosphorylation of the downstream AKT substrate GSK3. (*c*) Xanthohumol binds with AKT. (*d*, *e*) Xanthohumol inhibits AKT1 or AKT2 activity in an ATP-dependent manner. (*f*) Xanthohumol binds with AKT1 (*upper left*); enlarged view of the binding (*upper right*). Xanthohumol binds with AKT2 (*lower left*); enlarged view of the binding (*lower right*). AKT1/2 structures are shown as ribbon representation and xanthohumol is shown in stick representation with hydrogen bonds shown as red lines. [Color figure can be viewed at wileyonlinelibrary.com]

Preparation of AKT1/2 knockdown cells

For knocking down the expression of AKT1/2 in ESCC cells, the pLKO.1-mock, shRNA-Akt1 or shRNA-Akt2 plasmids together with packaging vectors, pMD2.0G and psPAX (Addgene Inc., Cambridge, MA) were transfected into 293T cells using the Simple-Fect transfection reagent (Signaling Dawn Biotech, Wuhan, Hubei, China) following the manufacturer's protocols. The transfection medium was changed at 12 hr and then cells were cultured for another 48 hr. The viral particles were harvested by filtration using a 0.45 μm syringe filter. KYSE70, KYSE450, or KYSE510 cells were treated with a mixture of polybrene and mock or AKT1/2 viral particles. Then 24 hr later, cells were treated with puromycin to select

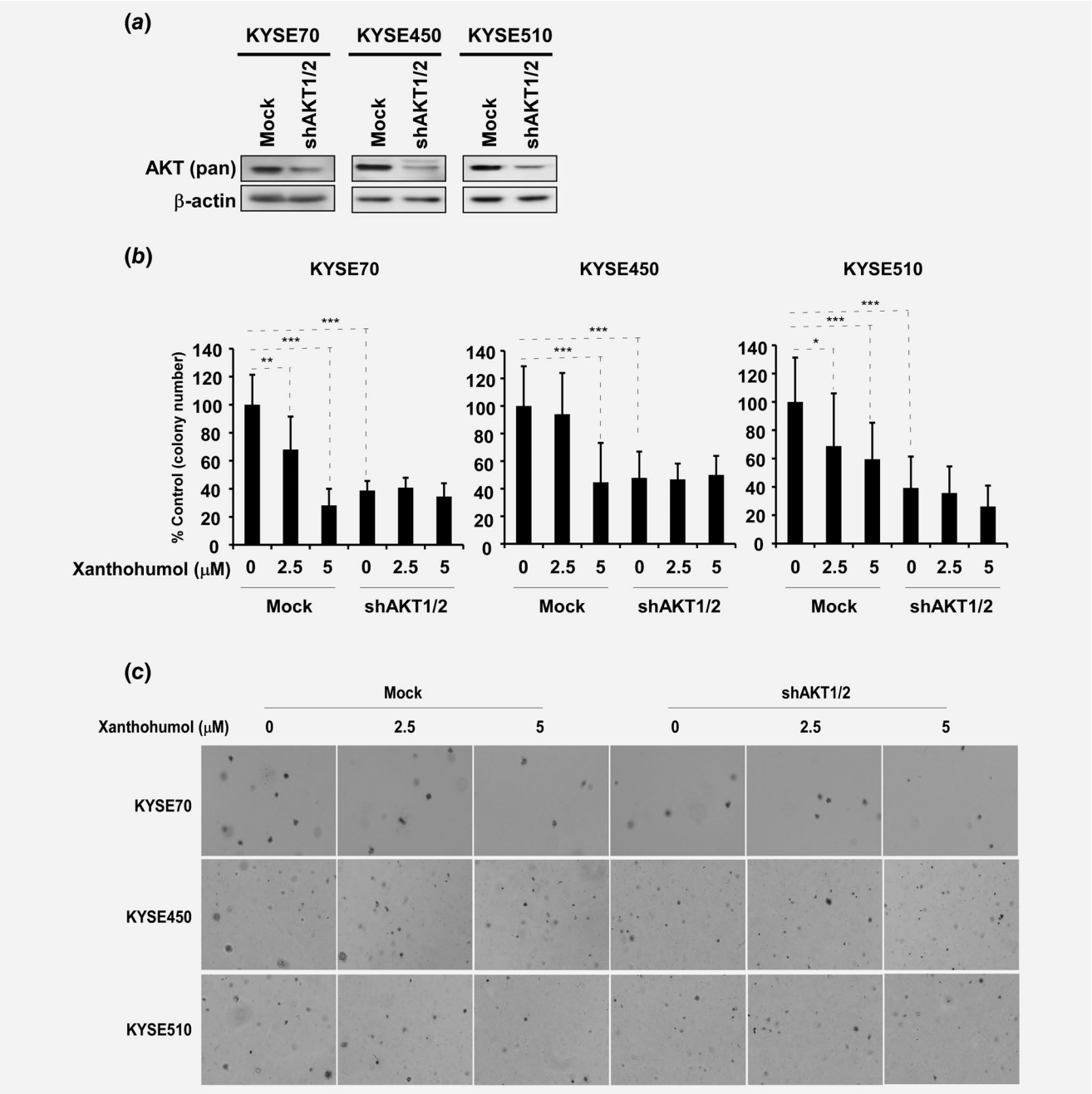

Figure 3. AKT1/2 knockdown suppresses colony formation of ESCC cells. (*a*) AKT1/2 expression was knocked down in KYSE70, 450 and 510 ESCC cell lines. (*b*) Anchorage-independent cell growth is decreased with or without xanthohumol treatment after AKT1/2 expression was decreased. (c) Representative colony pictures after AKT1/2 silenced with or without xanthohumol treatment. Asterisks (*$p < 0.05$, **$p < 0.01$, ***$p < 0.001$) indicate a significant decrease in colony formation of ESCC cells.

AKT1/2 knockdown cells. After AKT1/2 knockdown, the cells were used for the anchorage-independent cell growth assay and Western blot analysis.

PDX animal experiment

Six- to eight-week-old severe combined immunodeficient (SCID) female mice (Vital River Labs., Beijing, China) were used for animal experiments. This study was approved by the Ethics Committee of Zhengzhou University (Zhengzhou, Henan, China). We studied 3 cases of ESCC in PDX animal experiments designated as EG9, HEG5, or HEG18. PDX tumor masses were inoculated into SCID mice. When tumors reached an average volume of about 100 mm^3, mice were divided into 3 groups for further experiments as follows: (*i*) vehicle-treated group (n = 10–12); (*ii*) group treated with 80 mg/kg of xanthohumol (n = 10–12); and (*iii*) group treated with 160 mg/kg of xanthohumol (n = 10–12). Xanthohumol was

administered to the mice by gavage once a day for 50 days. Tumor volume was calculated from measurements of 3 diameters of the individual tumor base using the following formula: tumor volume (mm^3) = (length × width × height × 0.52). Mice were monitored until tumors reached 1.0 cm^3 total volume, at which time mice were euthanized and tumors extracted.

Immunohistochemical analysis

Tumor tissues embedded in paraffin were subjected to hematoxylin and eosin (H&E) staining and immunohistochemistry (IHC). Tissue samples were deparaffinized and hydrated and permeabilized with 0.5% Triton X-100 in 1× phosphate buffered saline (PBS) for 10 min. Then the sections were incubated at 4°C overnight with antibodies to detect Ki-67, p-AKT, p-GSK3β, p-mTOR, or p-S6K. The sections were washed 3 times with 1× PBS and incubated with the appropriate secondary antibodies. 3,3′-Diaminobenzidine was used to visualize the target proteins and then counterstained with hematoxylin. After staining, the sections were photographed (100X magnification) and analyzed using the Image-Pro Plus software (v.6.0) program (Media Cybernetics, Rockville, MD).

Statistical analysis

All quantitative results are expressed as mean values ± SD. For comparative analysis, a two-tailed independent sample *t*-test was used to determine differences among groups, and p value of <0.05 was considered as a statistically significant difference.

Results

Xanthohumol inhibits proliferation of ESCC cancer cells and induces apoptosis and cell cycle arrest at the G1 phase

In order to evaluate the threshold value between therapeutic dose and toxicity against normal cells, we first determined the effect of xanthohumol on growth of normal SHEE esophageal cells. After 72 hr of treatment, cell viability decreased more than 20%, which illustrates the toxicity of xanthohumol against the SHEE cell line at a concentration of 10 μM. Therefore, we selected the nontoxic concentration range of xanthohumol of 0–5 μM for further study (Supporting Information Fig. S1A). Xanthohumol treatment significantly inhibited cell proliferation in a concentration-dependent manner and the inhibitory effects at 5 μM xanthohumol are approximately 70, 70 or 80%, respectively, against KYSE70, 450 or 510 ESCC cells (Fig. 1*a*). In an anchorage-independent cell growth assay, xanthohumol showed inhibitory effects consistent with its suppressive effects on cell proliferation in these cell lines (Fig. 1*b*). Colony number and size were also significantly decreased (more than 50%) after treatment with xanthohumol compared to DMSO-treated cells (Fig. 1*b*; Supporting Information Fig. S1B).

After treatment of KYSE70, KYSE450 or KYSE510 cell lines with xanthohumol, cyclin D1 expression, which is a cell cycle marker at G1 phase, was decreased (Fig. 1*c*; Supporting Information Fig. S2A). The result was confirmed by staining with propidium iodide (PI). Arrest of cell cycle at the G1 phase was induced in xanthohumol-treated cells compared to DMSO-treated control cells (Fig. 1*d*). Statistical analysis of apoptosis data was based on the summary of annexinV+/PI+ gating (total apoptosis). The average percentage of total apoptosis was increased by 20, 24 or 21%, respectively, with 5 μM xanthohumol-treatment including annexinV+/PI− gating (early apoptosis) percentage of 14, 10 or 9%, respectively (Fig. 1*e*; Supporting Information Fig. S2B). To further confirm the effects of xanthohumol on apoptosis, we conducted Western blotting to detect expression of apoptosis biomarkers after xanthohumol treatment. Xanthohumol indeed induced expression of apoptosis biomarkers, including cleaved PARP, cleaved Caspase 3, cleaved

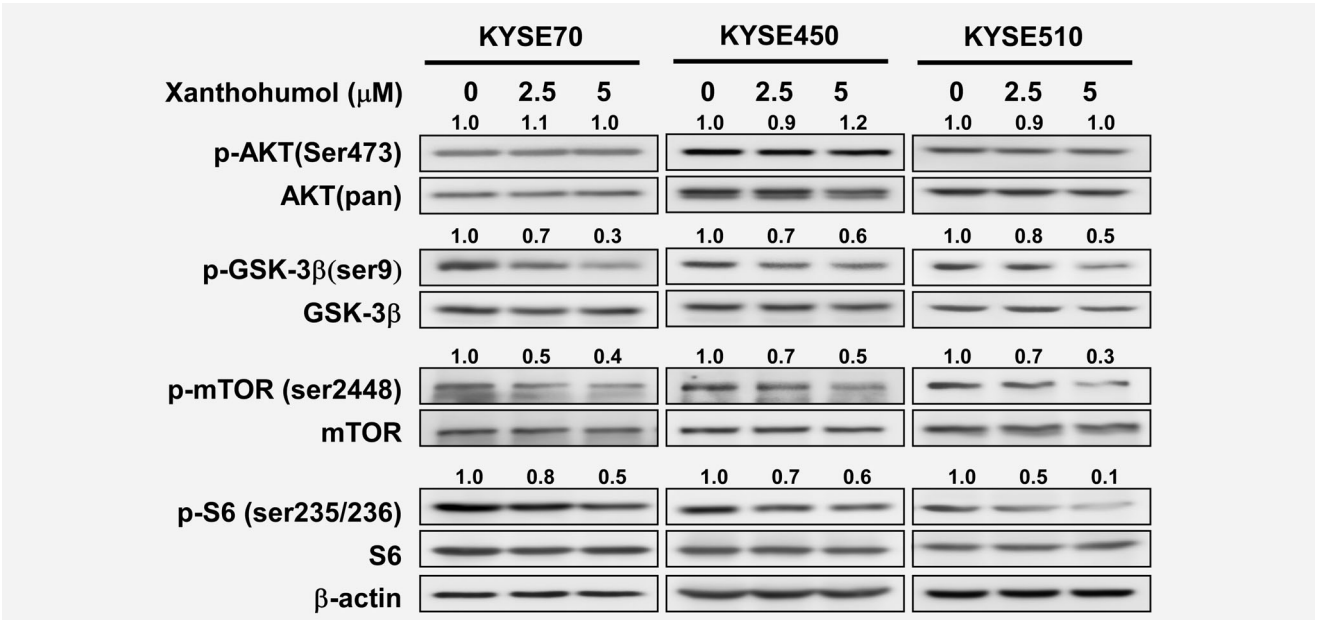

Figure 4. Xanthohumol downregulates AKT-related signaling pathways. Treatment with xanthohumol for 3 hr has no effect on p-AKT expression but downregulates p-GSK3β, p-mTOR and p-S6K. Western blot data are quantified and shown relative to corresponding total protein levels.

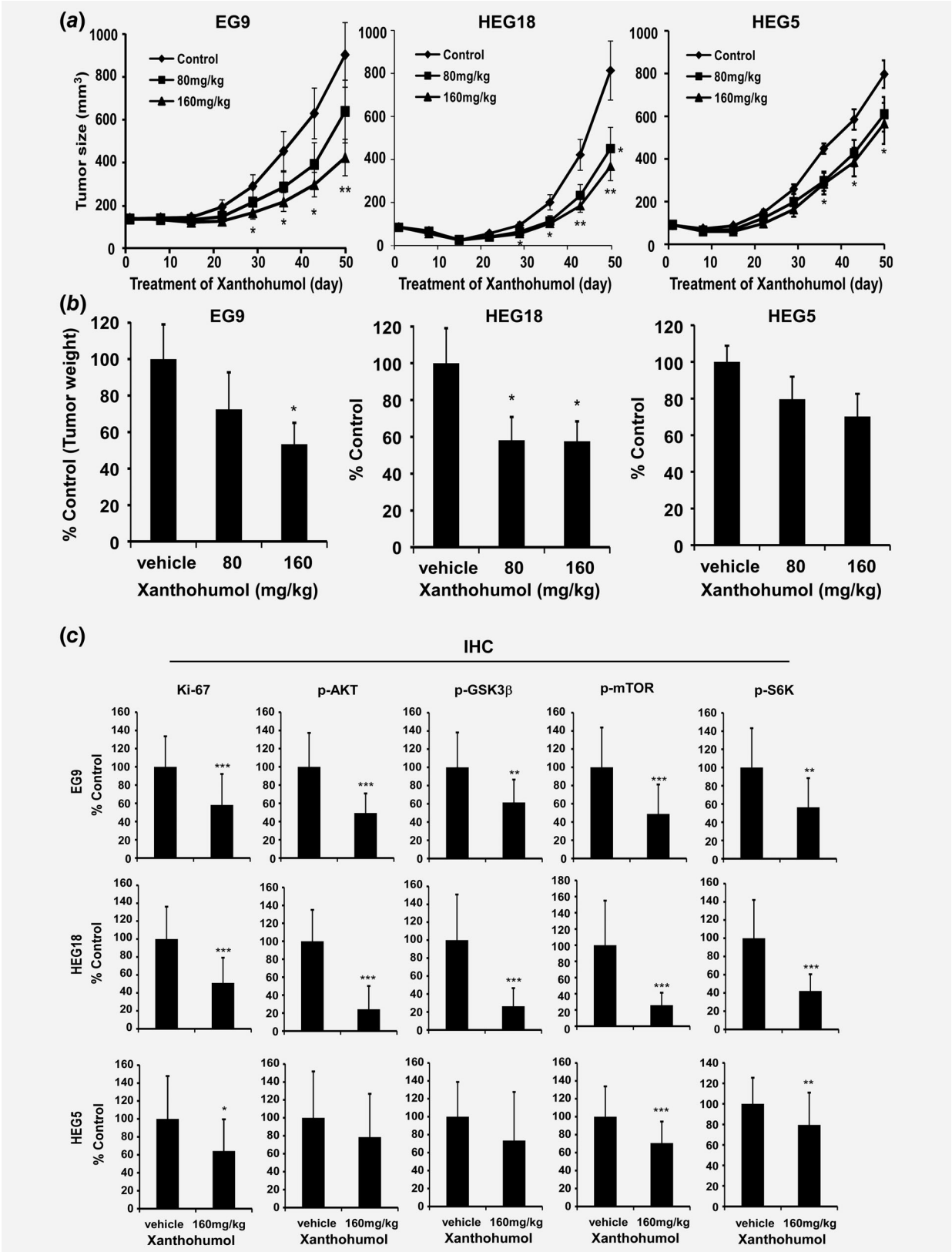

Figure 5. Legend on next page.

Caspase 7, Bax and Bim_s (Fig. 1*f*). Also xanthohumol increased extrinsic apoptosis marker death receptors (DR) 4 and 5 (Fig. 1*g*) as well as intrinsic apoptosis marker cytochrome c in mitochondria (Fig. 1*h*).

Xanthohumol inhibits AKT1/2 kinase activity

In order to study the inhibitory mechanism of xanthohumol in ESCC cell growth, we determined the direct target of xanthohumol by kinase profiling analysis (Supporting Information Figs. S3A and S3B). Next, we conducted an *in vitro* kinase assay with the active form of AKT1 or AKT2 to determine whether AKT kinase activity is a target of xanthohumol (Figs. 2*a* and 2*b*). The results showed that xanthohumol at 0.6–1.25 μM inhibited AKT kinase activity thereby suppressing the phosphorylation of its substrate, GSK3β (Figs. 2*a* and 2*b*). We then conducted an *ex vivo* pull-down assay with a KYSE510 cell lysate and found that xanthohumol bound with AKT (Fig. 2*c*). To determine whether the binding between xanthohumol and AKT occurred at the ATP pocket, we performed an ATP and xanthohumol competitive binding assay (Figs. 2*d* and 2*e*). The binding of xanthohumol to AKT1 or AKT2 decreased with increasing concentrations of ATP, suggesting that the compound binds at the ATP pocket and competes for ATP (Figs. 2*d* and 2*e*). To illustrate how xanthohumol interacts with AKT1 or AKT2, we created a computational model by docking xanthohumol *in silico* to the ATP binding pocket of AKT1 or AKT2. From the docking results, we found that xanthohumol formed hydrogen bonds at Ala230, Glu228, Glu234 and Lys158 in the backbone of AKT1 (Fig. 2*f*, *upper panel*) and at Glu236, Thr213 and Lys181 of AKT2, respectively (Fig. 2*f*, *lower panel*). We also found that xanthohumol could bind with PDK1 and p70S6K (Supporting Information Fig. S3B). The kinase assay data from PDK1 and p70S6K indicated that xanthohumol inhibited these kinase activities at 2.5 μM, suggesting that AKT is the primary target (Supporting Information Figs. S3C and S3D).

We examined p-AKT and AKT expression in normal esophageal cells and different ESCC cell lines (Supporting Information Fig. S4). Based on the results, we selected cell lines KYSE70, 450 and 510, which had the highest AKT expression levels, to conduct further studies. Moreover, we prepared AKT knockdown cells by infecting cells with virus particles containing shRNA-mock or shRNA-AKT1/2 (Fig. 3*a*) and then conducted the anchorage-independent cell growth assay (Figs. 3*b* and 3*c*). Knockdown of AKT1/2 in ESCC cells resulted in decreased colony formation of about 60% compared to mock-infected cells (Figs. 3*b* and 3*c*). However, treatment with xanthohumol failed to further inhibit colony formation in shRNA-AKT1/2 cells (Figs. 3*b* and 3*c*).

Xanthohumol regulates AKT downstream signaling pathways

Because AKT is a target of xanthohumol, we investigated the effects of xanthohumol treatment on AKT downstream signaling pathways. Cells treated with vehicle, 2.5 or 5 μM xanthohumol showed no change in expression of phosphorylated AKT or total AKT levels; however, phosphorylation of GSK3β, mTOR and ribosomal protein S6, which are downstream targets, was diminished with 2.5 or 5 μM xanthohumol treatment compared to vehicle-treated cells (Fig. 4).

Xanthohumol inhibits tumor growth of PDXs

In order to confirm the inhibitory effect of xanthohumol *in vivo*, we chose three patient cases to create PDX models and conduct further studies (Fig. 5; Supporting Information Fig. S5A). In the cases of EG9 and HEG18, the AKT expression level was higher compared to that in normal esophageal tissue (Supporting Information Fig. S5B). In these two cases, xanthohumol significantly inhibited tumor growth without loss of body weight compared to vehicle control group (Figs. 5*a* and 5*b*; Supporting Information Figs. 5C,D). The AKT expression of the HEG5 case was lower than that of EG9 and HEG18 cases. In this case, the tumor weight decreased around 30% after treatment with 160 mg/kg xanthohumol, whereas the EG9 or HEG18 case showed about a 50% decrease in growth. The expression of p-AKT and AKT in the HEG18 case was higher than that in EG9, and in this case, treatment with 80 mg/kg xanthohumol also showed a 50% decrease in tumor weight. These results indicate that inhibition of tumor volume and weight with xanthohumol treatment is dependent on the expression level of AKT (Figs. 5*a* and 5*b*).

Ki-67 is a nuclear protein that is associated with cell proliferation and ribosomal RNA transcription.[30] Ki-67 was present in all active phases of cell cycle, but absent from resting cells.[31] The prognostic value of Ki-67 for survival and tumor recurrence have been confirmed in some cancer types, such as breast cancer, prostate cancer and neuroendocrine cancer.[32–34] It also shows prognostic potential in ESCC.[35] Therefore, we detected the Ki-67 expression level in ESCC to determine if xanthohumol can affect its expression. AKT and its downstream proteins have also been examined by immunohistochemical analysis. The immunohistochemical analysis results showed that the xanthohumol-treated groups had decreased expression of Ki-67, p-AKT, p-GSK3β, p-mTOR or p-S6K by approximately 50 and 70% in the EG9 and HEG18 cases, respectively, compared to the vehicle-treated group (Fig. 5*c*; Supporting Information Fig. 6). The staining ratio of the markers in the HEG18 case was around 20% less than that in the EG9 case. In contrast, xanthohumol treatment induced an approximately 30% downregulation of Ki-67, p-AKT, p-GSK3β, p-mTOR and p-S6K in the

Figure 5. Xanthohumol has a chemopreventive effect on PDX tumor growth. (*a*) Tumor volume is decreased after xanthohumol treatment. (*b*) Tumor weight is decreased after xanthohumol treatment. Data are shown as each treatment group compared to the control group. Statistical significance was determined using a two-tailed independent sample *t*-test. Asterisks (*$p < 0.05$, **$p < 0.01$) indicate a significant decrease in tumor growth. (*c*) Quantitation of protein expression from IHC positive staining. Values are quantified from IHC staining and expressed as treatment group compared to vehicle-treated control group. Asterisks (*$p < 0.05$, **$p < 0.01$, ***$p < 0.001$) indicate a significant decrease in IHC staining. Detailed information is shown in the "Materials and Methods" section.

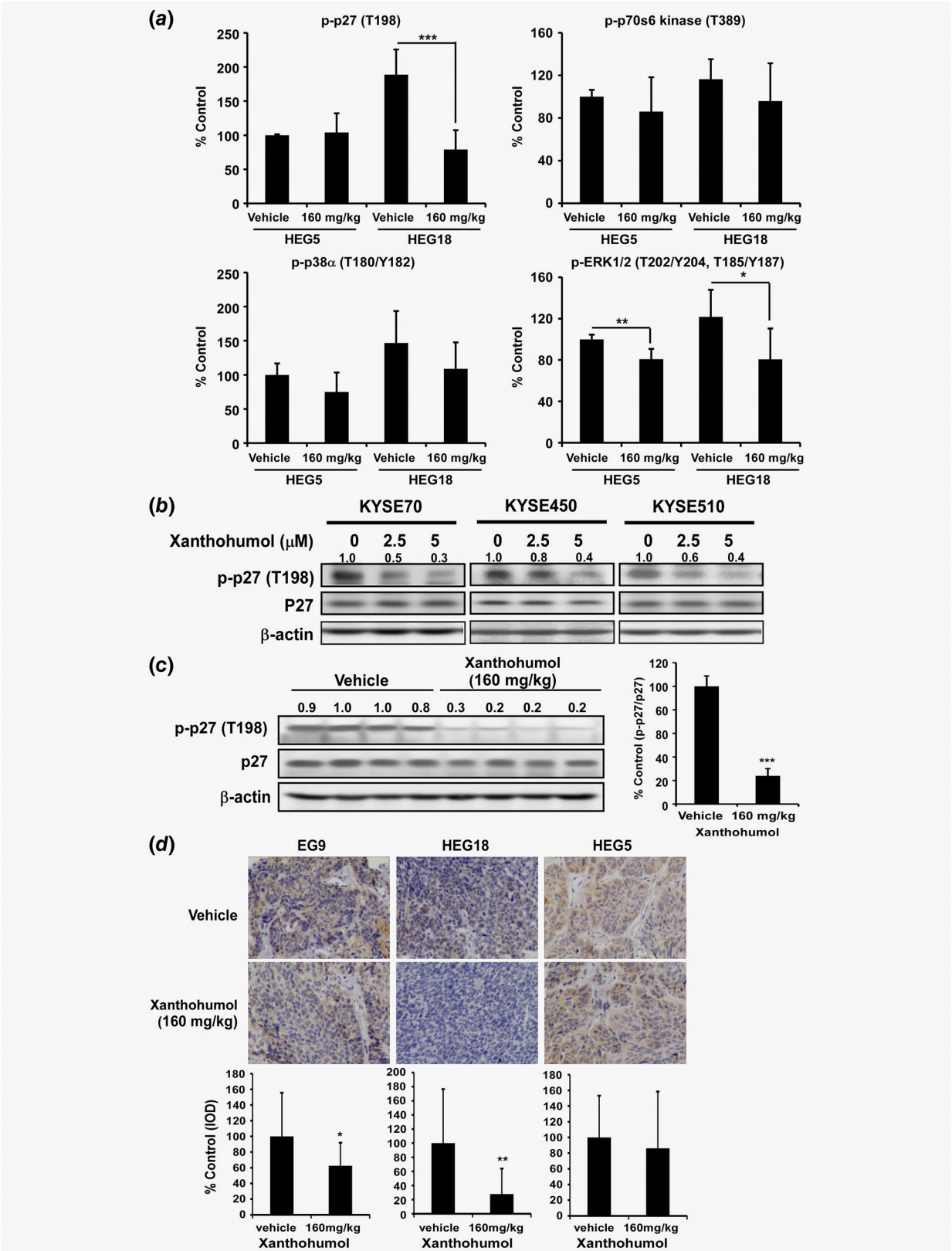

Figure 6. Legend on next page.

HEG5 case; however, this was not as obviously decreased compared to the EG9 (50%) and HEG18 (70%) cases (Fig. 5*c*).

Xanthohumol inhibits p-p27 expression

The PDX cases we chose were based on the expression level of p-AKT and AKT. From the therapeutic data of the PDX model, we found that the HEG18 case is more sensitive than HEG5. Although we found decreases in the phosphorylation of several AKT-associated proteins xanthohumol treatment (Fig. 5*c*; Supporting Information Fig. 5E), we are still not sure whether other pathways participate in the xanthohumol therapeutic effects. In order to determine whether other protein targets were involved in the enhanced therapeutic effects exerted by xanthohumol, we examined changes in phosphorylated kinases by comparing PDX samples from HEG5 and HEG18 cases that were treated with vehicle or xanthohumol (160 mg/kg). Based on the human phosphokinase array results, p-p27, p-p38α and p-ERK1/2 decreased more in the HEG18 case compared to the HEG5 case (Fig. 6*a*). In particular, p-p27 was downregulated substantially in the HEG18 case, but was not changed in the HEG5 case, indicating that p27 might be another targeted effect exerted by xanthohumol treatment. The p27 protein is a cell cycle regulator and tumor suppressor that participates in many cellular events. It functions by negatively regulating G1/S cell cycle progression and is also involved in apoptosis and autophagy as well as resistance to therapy. Some cancer types, such as colon cancer, lung cancer and esophageal cancer, showed decreased expression of p27.[36] The p27 protein is reported as a downstream target of AKT that can be phosphorylated by AKT at Thr198.[37,38] According to the kinase array results, we hypothesized that p27 plays a role in the enhanced therapeutic effects of xanthohumol. Therefore, we examined the phosphorylation of p27 in cell lines and tumor tissues. After xanthohumol treatment, p-p27 (Thr198) expression level was downregulated in the KYSE70, KYSE450 or KYSE510 cell lines (Fig. 6*b*). Additionally, in the HEG18 case, the p-p27 (Thr198) expression level was sharply decreased in the xanthohumol-treated group compared to the vehicle-treated group (Fig. 6*c*). The p-p27 expression level was downregulated in the EG9, HEG18 and HEG5 cases by 37, 72 and 14% as determined by immunohistochemical analysis (Fig. 6*d*).

Discussion

AKT kinase activity is commonly deregulated in many human tumor types and can be activated by hormones and some growth factors.[39,40] Activation of AKT will mainly induce phosphorylation of mTOR and GSK3β signaling pathways ultimately leading to increased proliferation and survival of cancer cells. Given the oncogenic characteristics of AKT, inhibitors are needed to prevent its phosphorylation and activation. Several selective AKT inhibitors, including MK2206, GSK2141795 and GSK690693, are undergoing clinical trials against different types of cancer. Identification of new, effective AKT inhibitors, and especially natural compound inhibitors, might improve the therapeutic effects against cancer by treatment alone or in combination with clinical drugs.

Xanthohumol was reported to attenuate lung and breast cancer cell growth and the anticancer effects of xanthohumol were associated with the downregulation of EGFR, STAT3, Notch and nuclear factor-κB (NF-κB).[21,41,42] However, the mechanisms underlying its chemopreventive/therapeutic effects remain unresolved. The present study focused on identifying a direct target of xanthohumol and we found that xanthohumol inhibited AKT kinase activity (Figs. 2*a* and 2*b*). ATP competitive binding and docking model (Figs. 2*d* and 2*e*) results illustrated that xanthohumol is an ATP competitive AKT kinase inhibitor. AKT plays an important role in cell proliferation, survival and metastasis[13,16] and it is a promising therapeutic target against cancer.[14] In this study, we found that p-AKT is overexpressed in cancer tissues compared to adjacent tissues. Knockdown of AKT1/2 in ESCC cells led to decreased colony formation (Figs. 3*b* and 3*c*). Considering that AKT kinase activity is a target of xanthohumol, we examined ESCC proliferation after treatment with the commercially available AKT inhibitor, MK2206. MK2206 inhibited growth of KYSE70, KYSE450 and KYSE510 cells in a dose-dependent manner from 0.3 to 10 μM (Supporting Information Fig. 7). Compared to MK2206, xanthohumol (5 μM) showed a similar inhibitory effect (approximately 70%) with 10 μM MK2206 at 72 hr. After AKT1/2 knockdown, xanthohumol failed to further suppress colony formation (Fig. 3*b*). These data indicate that AKT is a primary target of xanthohumol.

PDX models are used to screen for biomarkers and predict clinical trial drug response because of the stable biological and genetic characteristics from the patient donor tumor. PDX models are ideal models for translational medical research. Therefore, the evaluation of xanthohumol's chemopreventive effect in PDX models was an essential part of this study. We compared the chemopreventive effects of xanthohumol based on the AKT expression level. From our data, PDX tumors exhibiting higher AKT expression levels had more dramatic decreases in tumor volume and weight as well as related IHC biomarker staining (Figs. 5*a* and 5*c*; Supporting Information Figs. S5C and S6) when treated with xanthohumol. Other types of cancers could also be established as PDX models on the basis of AKT expression level and could be

Figure 6. Xanthohumol inhibits AKT downstream p27 kinase expression. (*a*) p-p27 decreased more in the HEG18 PDX tumor compared to the HEG5 PDX tumor. It was also more substantially decreased compared to p-p38α, p-ERK1/2, or p-p70s6 kinase as determined by a human phosphor-kinase array. (*b*) The p-p27 protein expression level is decreased in ESCC cell lines after xanthohumol treatment. (*c*) The p-p27 protein expression level in the HEG18 PDX tumor (*left panel*). Four samples were selected from the vehicle group and the group treated with 160 mg/kg xanthohumol group, respectively. Data (*right panel*) are shown as quantification of the average p-p27 expression level divided by total p27 expression setting the vehicle group as 100%. (*d*) Statistical analysis of IHC positive staining of p-p27 (Thr198) and representative IHC photographs of HEG5, EG9 and HEG18. Values are quantified from IHC staining and expressed as the treatment groups compared to the control group. Asterisks (*$p < 0.05$, **$p < 0.01$, ***$p < 0.001$) indicate a significant change. [Color figure can be viewed at wileyonlinelibrary.com]

used for effective AKT inhibitor screening. PDX models can supply important information for the translation from preclinical studies to clinical studies.

The p27 protein is a negative regulator of cell cycle progression and belongs to the Cip/Kip family. Post-translational modification of p27 is the primary mode of its regulation. The localization of p27 determines its various functions. In the nucleus, p27 inhibits cell proliferation, but enhances cell motility.[37,38,43,44] It is reportedly phosphorylated by AKT at Thr198. In our study, we found that the p-p27 expression level was downregulated in KYSE70, KYSE450 or KYSE510 cell lines, as well as in PDX tumors developed from the HEG18 case (Figs. 6*b* and 6*c*). The inhibitory effect of xanthohumol on p-p27 was enhanced in the AKT-highly expressing HEG18 case compared to the HEG5 case, suggesting that the therapeutic effect of xanthohumol is likely involved in the AKT-p27 signaling pathway.

In the current study, we found that xanthohumol inhibited AKT kinase activity by negatively regulating the phosphorylation of the AKT substrate, GSK3β, which resulted in growth inhibition, apoptosis induction and cell cycle arrest in ESCC cell lines that highly express AKT. In PDX *in vivo* models, xanthohumol therapy induced tumor regression by targeting AKT and the AKT expression level was associated with the therapeutic effect of xanthohumol. This study provides information useful for moving xanthohumol toward the clinic and shows the prospective translational potential of xanthohumol for ESCC patients with high expression levels of AKT.

Acknowledgements

We wish to thank Shen Yang, China-US (Henan) Hormel Cancer Institute for supporting experiments. This work was supported by grant funding from the National Institute of Health (NIH), USA, CA187027 and CA 196639; the Key Program of Henan Province, China, Grant No. 161100510300 (to Z. Dong); the National Natural Science Foundation of China NSFC81672767 (to M. Lee) and No. 81802875 (to X. Liu) and Henan Provincial Government, China.

References

1. Song Y, Li L, Ou Y, et al. Identification of genomic alterations in oesophageal squamous cell cancer. *Nature* 2014;509:91–5.
2. Smyth EC, Lagergren J, Fitzgerald RC, et al. Oesophageal cancer. *Nat Rev Dis Primers* 2017;3: 17048.
3. Pan R, Zhu M, Yu C, et al. Cancer incidence and mortality: a cohort study in China, 2008-2013. *Int J Cancer* 2017;141:1315–23.
4. Chen W, Zheng R, Baade PD, et al. Cancer statistics in China, 2015. *CA Cancer J Clin* 2016;66:115–32.
5. Konishi H, Fujiwara H, Shiozaki A, et al. Effects of neoadjuvant 5-fluorouracil and cisplatin therapy in patients with clinical stage II/III esophageal squamous cell carcinoma. *Anticancer Res* 2018;38:1017–23.
6. Werner D, Atmaca A, Pauligk C, et al. Phase I study of everolimus and mitomycin C for patients with metastatic esophagogastric adenocarcinoma. *Cancer Med* 2013;2:325–33.
7. Hiramoto S, Kato K, Shoji H, et al. A retrospective analysis of 5-fluorouracil plus cisplatin as first-line chemotherapy in the recent treatment strategy for patients with metastatic or recurrent esophageal squamous cell carcinoma. *Int J Clin Oncol* 2018;23:466–72.
8. Chen J, Su T, Lin Y, et al. Intensity-modulated radiotherapy combined with paclitaxel and platinum treatment regimens in locally advanced esophageal squamous cell carcinoma. *Clin Transl Oncol* 2018;20:411–9.
9. Nakamura K, Kato K, Igaki H, et al. Three-arm phase III trial comparing cisplatin plus 5-FU (CF) versus docetaxel, cisplatin plus 5-FU (DCF) versus radiotherapy with CF (CF-RT) as preoperative therapy for locally advanced esophageal cancer (JCOG1109, NExT study). *Jpn J Clin Oncol* 2013;43:752–5.
10. Ku GY. Systemic therapy for esophageal cancer: chemotherapy. *Chin Clin Oncol* 2017;6:49.
11. Lyons TG, Ku GY. Systemic therapy for esophagogastric cancer: targeted therapies. *Chin Clin Oncol* 2017;6:48.
12. Paraskevopoulou MD, Tsichlis PN. A perspective on AKT 25-plus years after its discovery. *Sci Signal* 2017;10:eaan8791.
13. Vara JÁF, Casado E, de Castro J, et al. PI3K/Akt signalling pathway and cancer. *Cancer Treat Rev* 2004;30:193–204.
14. Pal I, Mandal M. PI3K and Akt as molecular targets for cancer therapy: current clinical outcomes. *Acta Pharmacol Sin* 2012;33:1441–58.
15. Song M, Liu X, Liu K, et al. Targeting AKT with oridonin inhibits growth of esophageal squamous cell carcinoma in vitro and patient-derived xenografts in vivo. *Mol Cancer Ther* 2018;17:1540–53.
16. Li B, Xu WW, Lam AKY, et al. Significance of PI3K/AKT signaling pathway in metastasis of esophageal squamous cell carcinoma and its potential as a target for anti-metastasis therapy. *Oncotarget* 2017;8:38755–66.
17. Hidalgo M, Amant F, Biankin AV, et al. Patient-derived xenograft models: an emerging platform for translational cancer research. *Cancer Discov* 2014;4:998–1013.
18. Gao H, Korn JM, Ferretti S, et al. High-throughput screening using patient-derived tumor xenografts to predict clinical trial drug response. *Nat Med* 2015;21:1318–25.
19. Ji X, Chen S, Guo Y, et al. Establishment and evaluation of four different types of patient-derived xenograft models. *Cancer Cell Int* 2017;17:122.
20. Contreras-Zarate MJ, Ormond DR, Gillen AE, et al. Development of novel patient-derived xenografts from breast cancer brain metastases. *Front Oncol* 2017;7:252.
21. Zou J, Liu Y, Wang J, et al. Establishment and genomic characterizations of patient-derived esophageal squamous cell carcinoma xenograft models using biopsies for treatment optimization. *J Transl Med* 2018;16:15.
22. Pillai SG, Li S, Siddappa CM, et al. Identifying biomarkers of breast cancer micrometastatic disease in bone marrow using a patient-derived xenograft mouse model. *Breast Cancer Res* 2018; 20:2.
23. Risbridger GP, Toivanen R, Taylor RA. Preclinical models of prostate cancer: patient-derived xenografts, organoids, and other explant models. *Cold Spring Harb Perspect Med* 2018;8.
24. Weiskirchen R, Mahli A, Weiskirchen S, et al. The hop constituent xanthohumol exhibits hepatoprotective effects and inhibits the activation of hepatic stellate cells at different levels. *Front Physiol* 2015;6:140.
25. Slawinska-Brych A, Zdzisinska B, Dmoszynska-Graniczka M, et al. Xanthohumol inhibits the extracellular signal regulated kinase (ERK) signalling pathway and suppresses cell growth of lung adenocarcinoma cells. *Toxicology* 2016;357-358: 65–73.
26. Azevedo C, Correia-Branco A, Araujo JR, et al. The chemopreventive effect of the dietary compound kaempferol on the MCF-7 human breast cancer cell line is dependent on inhibition of glucose cellular uptake. *Nutr Cancer* 2015;67:504–13.
27. Zhao X, Jiang K, Liang B, et al. Anticancer effect of xanthohumol induces growth inhibition and apoptosis of human liver cancer through NF-kappaB/p53-apoptosis signaling pathway. *Oncol Rep* 2016;35:669–75.
28. Shen ZY, Xu LY, Li EM, et al. Immortal phenotype of the esophageal epithelial cells in the process of immortalization. *Int J Mol Med* 2002;10: 641–6.
29. Schrödinger. *Schrödinger Suite 2015 ed.* New York, NY: LLC, 2015.
30. Bullwinkel J, Baron-Luhr B, Ludemann A, et al. Ki-67 protein is associated with ribosomal RNA transcription in quiescent and proliferating cells. *J Cell Physiol* 2006;206:624–35.
31. Bruno S, Darzynkiewicz Z. Cell cycle dependent expression and stability of the nuclear protein detected by Ki-67 antibody in HL-60 cells. *Cell Prolif* 1992;25:31–40.
32. Acs B, Zambo V, Vizkeleti L, et al. Ki-67 as a controversial predictive and prognostic marker in breast cancer patients treated with neoadjuvant chemotherapy. *Diagn Pathol* 2017;12:20.
33. Berlin A, Castro-Mesta JF, Rodriguez-Romo L, et al. Prognostic role of Ki-67 score in localized prostate cancer: a systematic review and meta-analysis. *Urol Oncol* 2017;35:499–506.
34. Nielsen LAG, Bangso JA, Lindahl KH, et al. Evaluation of the proliferation marker Ki-67 in

gliomas: interobserver variability and digital quantification. *Diagn Pathol* 2018;13:38.
35. Deng HY, Chen ZH, Wang ZQ, et al. High expression of Ki-67 is an independent favorable prognostic factor for esophageal small cell carcinoma. *Oncotarget* 2017;8:55298–307.
36. Chu IM, Hengst L, Slingerland JM. The Cdk inhibitor p27 in human cancer: prognostic potential and relevance to anticancer therapy. *Nat Rev Cancer* 2008;8:253–67.
37. Fujita N, Sato S, Katayama K, et al. Akt-dependent phosphorylation of p27Kip1 promotes binding to 14-3-3 and cytoplasmic localization. *J Biol Chem* 2002;277:28706–13.
38. Kim J, Jonasch E, Alexander A, et al. Cytoplasmic sequestration of p27 via AKT phosphorylation in renal cell carcinoma. *Clin Cancer Res* 2009;15:81–90.
39. Nicholson KM, Anderson NG. The protein kinase B/Akt signalling pathway in human malignancy. *Cell Signal* 2002;14:381–95.
40. Wang Q, Chen X, Hay N. Akt as a target for cancer therapy: more is not always better (lessons from studies in mice). *Br J Cancer* 2017;117:159–63.
41. Kang Y, Park MA, Heo SW, et al. The radiosensitizing effect of xanthohumol is mediated by STAT3 and EGFR suppression in doxorubicin-resistant MCF-7 human breast cancer cells. *Biochim Biophys Acta* 2013;1830:2638–48.
42. Sun Z, Zhou C, Liu F, et al. Inhibition of breast cancer cell survival by xanthohumol via modulation of the Notch signaling pathway in vivo and in vitro. *Oncol Lett* 2018;15:908–16.
43. Fujita N, Sato S, Tsuruo T. Phosphorylation of p27Kip1 at threonine 198 by p90 ribosomal protein S6 kinases promotes its binding to 14-3-3 and cytoplasmic localization. *J Biol Chem* 2003;278:49254–60.
44. Wang HC, Lee WS. Molecular mechanisms underlying progesterone-induced cytoplasmic retention of p27 in breast cancer cells. *J Steroid Biochem Mol Biol* 2018;183:202–9.